# OID: Outlier Identifying and Discarding in Blind Image Deblurring

Liang Chen[1], Faming Fang[1] *, Jiawei Zhang[2], Jun Liu[3], and Guixu Zhang[1]

[1] Shanghai Key Laboratory of Multidimensional Information Processing, School of Computer Science and Technology, East China Normal University
[2] SenseTime Research
[3] Key Laboratory of Applied Statistics of MOE, School of Mathematics and Statistics, Northeast Normal University
{liangchen527}@gmail.com, {fmfang}@cs.ecnu.edu.cn

**Abstract.** Blind deblurring methods are sensitive to outliers, such as saturated pixels and non-Gaussian noise. Even a small amount of outliers can dramatically degrade the quality of the estimated blur kernel, because the outliers are not conforming to the linear formation of the blurring process. Prior arts develop sophisticated edge-selecting steps or noise filtering pre-processing steps to deal with outliers (i.e. indirect approaches). However, these indirect approaches may fail when massive outliers are presented, since informative details may be polluted by outliers or erased during the pre-processing steps. To address these problems, this paper develops a simple yet effective Outlier Identifying and Discarding (OID) method, which alleviates limitations in existing Maximum A Posteriori (MAP)-based deblurring models when significant outliers are presented. Unlike previous indirect outlier processing methods, OID tackles outliers directly by explicitly identifying and discarding them, when updating both the latent image and the blur kernel during the deblurring process, where the outliers are detected by using the sparse and entropy-based modules. OID is easy to implement and extendable for non-blind restoration. Extensive experiments demonstrate the superiority of OID against recent works both quantitatively and qualitatively.

**Keywords:** Blind deblurring, Outliers, Identifying and discarding

## 1 Introduction

Single image blind deblurring is a well-known and ill-posed problem. It has drawn a lot of attention due to large requirements in digital image processing. Image blurring can be seen as a low-pass filtering process, resulting in distortion as well as irreversible degradation of high-frequency information in images such as edges and details [27]. Recent studies have shown promising results to deal with the deblurring problem [2, 3, 7, 8, 13, 14, 17, 18, 20, 23–25, 28–30], which mainly

* Corresponding Author

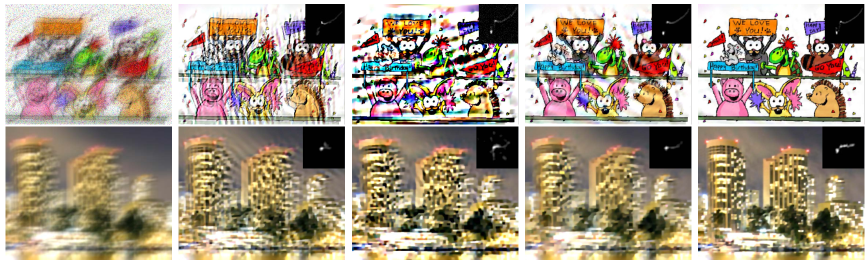

(a) Inputs (b) Chen et al. [2][4] (c) Pan et al. [22] (d) Dong et al. [5] (e) Ours

**Fig. 1.** Comparisons of deblurring results when outliers are presented. Inputs in the first and second rows contain impulsive noise and saturated pixels respectively. State-of-the-art method [2] is ineffective encounter outliers. Recent outlier handling methods [5,22] can ease the blur to some extent, but they are not as effective as our approach.

focus on two aspects including the MAP-based models that explore statistical priors for natural images, and other models that select informative edges. Despite the effectiveness of these methods, they are not able to recover blurred images that contain significant amounts of outliers, as presented in Fig. 1. The main reasons are that extracting edges in the presence of massive outliers is difficult, and outliers tend to violate the linear formation assumption of the blurring process [4,22] given by,

$$B = I \otimes K + \eta, \tag{1}$$

where $B, I, K$, and $\eta$ represent the blurred image, latent sharp image, blur kernel, and additive Gaussian noise, respectively. We use $\otimes$ to denote the convolution operator.

There are two main types of outliers remain to be solved, including non-Gaussian noise (e.g. impulsive noise) [1] and saturated pixels. Recent state-of-the-art outlier-handling models [5,22] develop sophisticated edge-selecting skills or designed specific fidelity term to cope with outliers. These techniques showed their effectiveness in many cases. However, when the informative edges in the images are difficult to extract, the edge-selecting approach will eventually fail (Fig. 1 (c)). In the meantime, specially designed fidelity functions may not be appropriate to fit the additive noise, which would lead to artifacts in the estimated latent images when the noise is not properly handled [25]. This explains the ineffectiveness of the method from [5] in the given examples (Fig. 1 (d)).

Instead of seeking useful edges or designing indirect functions to deal with outliers, we solve the problem by resorting to a more effective framework, namely outlier identifying and discarding (OID). To completely and precisely avoid the side-effect brought by outliers, OID explicitly targets at polluted elements in the fidelity term during the deblurring process and assigns predefined minimum values for these elements. In this way, outliers are guaranteed not to contribute within the MAP-framework. At the same time, the additive Gaussian noise can

[4] Note that the input with impulsive noise is preprocessed with Gaussian filter for this method before the deblurring process as reported in their paper.

still be properly fitted using an $l_2$ noise model. To be more specific, OID is integrated into both the updating steps of the latent image and the blur kernel in an iterative manner during the deblurring process. OID is capable of revealing potential outliers as well as neutralizing them during the deblurring process. Compared to prior arts, OID does not require complicated pre-processing steps or heuristic goodness-of-fit in function, and it enables massive outliers to be removed as shown in Fig. 1 (f). Extensive evaluations on benchmark datasets and real-world images demonstrate the superiority of OID against state-of-the-art outlier deblurring methods, especially when the blurred image contains significant outliers. The contributions of this work are three-fold.

- We propose outlier identifying and discarding (OID), a new strategy that iteratively identifies and discards outliers in both the processes of updating the latent image and the blur kernel. Further theoretical explanation validates the rationality of OID.
- OID employs continuous weights to indicate the probabilities of outliers, which can well target at polluted pixels without sacrificing a proper noise fitting model.
- OID can be effectively extended to the non-blind deblurring task. Extensive experiments demonstrate the superiority of OID against state-of-the-art methods in benchmark datasets and real-world blurry images.

## 2 Related Works

**Outlier-handling blind deblurring methods.** Many works [4–6, 10, 22, 26] have been proposed to deal with outliers in the deblurring task. We review some highly related blind deblurring approaches in this section.

Pan et al. [22] adopt a specially designed edge selecting strategy to find informative edges during image estimation step, and they also propose to cover more potentially polluted areas after outliers are detected. However, problems come with these strategies. When there exist massive outliers, selecting useful edges turns out to be quiet difficult, and this method tends to overcover unpolluted areas, leaving insufficient details to reveal the correct kernel. To avoid detecting outliers directly, Dong et al. [5] develop a sophisticated data fidelity term to suppress the side effect brought by outliers during deblurring steps. However, this scheme neglects the contribution of a decent noise fitting model, which will result in ringing artifacts in the estimated latent images [25]. In contrast to pioneer works, OID does not require any heuristic designs or strong regularization priors, and it shows comparable or even better performance confronting outliers.
**Outlier detection skills.** Locating outliers in the deblurring process is not as challenging as removing the side-effects brought by which. Intuitively, outliers are highly correlated with residuals between blurred images and convolution results of latent images and blur kernels: the higher the residuals values, the more likely the corresponding elements are outliers. In this work, we propose to indicate inliers and outliers in a more reliable approach. To be more specific, elements are not assigned with binary weights, but positive weights ranging

from 0 to 1, which can equally be viewed as probabilities of entries classified as inliers. To predict the probabilities more faithfully, we employ a maximum entropy regularization term, which serves to minimize the prediction bias [9]. The final sigmoid alike weighting function complies with the intuitional assumption, and it is replaceable with more potential outlier detecting methods.

## 3 Our Approach

In the real-world, blurry images are frequently degraded by other gross corruptions besides small additive noise. The most common degradations are saturated pixels and non-Gaussian noise [4]. While outliers often have significant effects on the goodness-of-fit in (1) [5], both the kernel and latent image updating processes will be misled by the incorrect elements in the fidelity term, the overall framework is destined to fail ultimately. Meanwhile, the edge selecting work may also fail since the edges of outliers are often more remarkable than inliers.

To make the MAP-based framework workable, a reasonable approach is to explicitly exclude the polluted elements in the fidelity term. This idea can be fulfilled by assigning different weights to elements: those classified as outliers are assigned with weights equal to zero to make sure they do not contribute to the deblurring process and vise versa for inliers. To avoid the overall optimization framework to be stuck in bad local minima, we propose to use a continuous weighting strategy instead of binary weights. The proposed strategy can also be viewed as classifying with probabilities.

With regularization terms imposed on the latent variables, the solutions can be obtained by optimizing the following equation,

$$\{I, K, W\} = \arg min \sum_i W_i |B_i - (I \otimes K)_i|^2 + R_I(I) + R_K(K) + R_W(W), \tag{2}$$

where $W$ denotes the weighting matrix, and $i$ represents pixel location; $R_I(\cdot)$, $R_K(\cdot)$ and $R_W(\cdot)$ are regularization terms imposed on latent images, blur kernels and weighting masks respectively. Here we use the $l_2$ norm to fit the additive noise same as the strategies from [2,19,23,29]. Compared to existing arts [5,22], the formulation of OID is more simple, and it enables the additive noise to be well modeled by an $l_2$ function. Taking the straightforward formation of OID, questions may be raised about its effectiveness. We show in the next subsection that this model can easily fail unless it is solved with a proper updating strategy.

### 3.1 Observations

**In this subsection, we show that locating outliers is not the only factor that leads to the success of OID. Different updating strategies will result in totally different results.** A naive approach to solve (2) is by updating the three variables in a sequence (i.e. $\{I, K, W\}$) until converge. This approach can be equally viewed as adding an outlier detecting step within the conventional MAP framework. However, this naive strategy has an intrinsic defect. Take the


(a) (b) (c) (d) (e) (f) (g)

**Fig. 2.** Illustration of the proposed updating strategy and a naive approach mentioned in Section 3.1. (a) Blurry input. (b)-(c) Intermediate outputs using the naive approach and the proposed strategy. (d)-(e) Detected outliers (dark pixels) corresponding to (b) and (c). (f)-(g) Outputs of the last updating sequence using the naive approach and the proposed strategy. The naive approach detects incorrect outliers with multiple useful edges, which accordingly leads to the failure case for the final results.

step of updating $I$ for example, every optimization step will lead to the change of the convolution output (i.e. $I \otimes K$). Consequently, the residual (i.e. $B - I \otimes K$) and the corresponding outlier information (i.e. $W$) change with the convolution output, because the outlier information is highly associated with the residual as mentioned in Section 2. Thus, the outdated outlier information is not applicable for the next updating step (i.e. updating $K$). As a result, the kernel misled by the incorrect outliers can be entirely different from the ground truth. Worse still, the overall deblurring process may fail with its output kernel in a delta function form. An example in Fig. 2 shows the limitation of this naive approach, where the detected outliers (Fig. 2 (d)) deviates from what is correct, and the overall process results in a delta kernel in the end (Fig. 2 (f)). More explanations of this strategy are presented in Section 4.1.

Based on the findings, we propose to remove the side-effects of outliers with a new updating approach. Especially, outliers should be re-identified in both steps of kernel and image updating processes, and they are calculated as soon as the latent variables (i.e. $I$ and $K$) are updated. Moreover, because the re-identified outliers may reversely lead to the change of the latent variables, we propose to iteratively update the latent variables and outliers until convergence. The overall updating strategy can be viewed as iteratively updating two inner loops (i.e. $\{\{W, I\}, \{W, K\}\},$). Note that with this strategy, the outliers can be initialized to be any value. The example shown in Fig. 2 illustrates the effectiveness of our observations, in which outliers in the blurry image are detected substantially correct (Fig. 2 (e)), and the final outputs (Fig. 2 (g)) are barely affected by the outliers. Additionally, we give an extensive explanation to validate the rationality of the proposed updating strategy in Section 4.1.

### 3.2 Proposed Method

Regularization terms for the image and blur kernel are not influential factors to the problem. For a fair comparison, we impose the hyper-Laplacian prior [15] on latent image the same as [5, 22], and we use a smooth constraint on the blur kernel for computational simplicity. As for the weighting mask (i.e. $W$), we assume that the corresponding classification probability should follow the maximum entropy rule [9], and outliers (i.e. elements with small weights) are sparse. The final OID model can be expressed as follows,

$$\begin{aligned}\min_{I,K,W} \sum_i W_i|B_i-(I\otimes K)_i|^2+\lambda\|\nabla I\|_{0.8}+\theta\|K\|_2^2+\alpha\|\overline{W}\|_1+\beta\sum_i(W_i\log W_i+\overline{W_i}\log\overline{W_i}),\\ \text{s.t.}\quad W_i+\overline{W_i}=1,\qquad \left\{W_i,\overline{W_i}\right\}\in[0,1]\,,\end{aligned}\tag{3}$$

where $\nabla$ denotes gradient operator in horizontal and vertical dimensions (i.e., $\nabla=\{\nabla_h,\nabla_v\}$); $\lambda$, $\theta$, $\alpha$ and $\beta$ are weighting parameters.

OID is developed to take advantage of clean elements while discarding elements polluted by outliers during the deblurring process, and it can benefit both kernel and latent image updating processes. Questions may be raised about the selection of sparse constraint on outliers. Although $l_0$ norm is ideal for hosting outliers, we use the $l_1$ norm in our formulation with reasonable modification and the computation complexity consideration. Please refer to our supplementary material for more illustrations.

### 3.3 Optimization

As described in Section 3.1, the optimization process of OID is carried out by iteratively minimizing following models,

$$\begin{cases}\min\limits_{I,W}\sum\limits_i W_i|B_i-(I\otimes K)_i|^2+R_I(I)+R_W(W), & (4)\\ \min\limits_{K,W}\sum\limits_i W_i|B_i-(I\otimes K)_i|^2+R_K(K)+R_W(W). & (5)\end{cases}$$

We solve (4) by alternatively updating $I$ and $W$ while fixing the other, and $K$ is fixed during the phase. We use the same updating strategy to solve (5). The overall process contains three individual optimization parts: the problems referring to update $I, K$ and $W$, respectively. We give a description for the optimization details in the following subsections.

**Optimizing the problem referring to *I*** While fixing $K$ and $W$, the problem referring to $I$ is given by,

$$\min_I \sum_i W_i|B_i-(I\otimes K)_i|^2+\lambda|(\nabla I)_i|^{0.8}.\tag{6}$$

We use the iteratively reweighted least squares (IRLS) method [15] to minimize (6) for simplicity. At each iteration, we have the following equation to solve,

$$\min_{I^t} \sum_i W_i|B_i-(I^t\otimes K)_i|^2+\lambda P_i|(\nabla I^t)_i|^2,\tag{7}$$

where $P_i=\min\{|(\nabla I^{t-1})_i|^{-1.2},\epsilon\}$, the constant $\epsilon$ here is used to prevent 0 in the denominator, and $t$ represents the iteration index. When $P_i$ are fixed, (7) becomes a quadratic function, and we can efficiently solve it with a conjugate gradient (CG) method. The whole process of IRLS can be seen as iteratively updating weights ($P_i$) and the latent image.

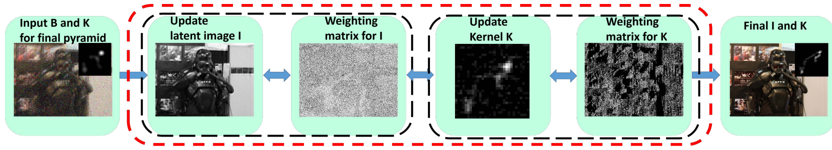


**Fig. 3.** Main steps of the proposed algorithm. The red and black dash lines denote outer and inner iteration during the process, respectively. Note the weight map in the kernel estimation step is different with which in the image updating step because it is calculated in the gradient domain. We only show the map in the horizontal dimension.

**Optimizing the problem referring to $\boldsymbol{K}$** To improve the accuracy of the estimated kernel [3, 25, 29], we replace the intensity domain in the data fidelity term by gradient domain. Removing the irrelevant terms, the blur kernel can be obtained by solving the following equation,

$$\min_{K} \sum_{i} W_i |(\nabla B - \nabla I \otimes K)_i|^2 + \theta \|K\|_2^2. \tag{8}$$

We use the CG method to solve the problem. We set its negative elements of $K$ to be 0 and normalize it after obtaining the kernel.

**Optimizing the problem referring to $\boldsymbol{W}$** Picking out the terms relevant to $W$ and $\overline{W}$ results in the following optimization problem,

$$\begin{gathered} \min_{W,\overline{W}} \sum_{i} W_i |B_i - (I \otimes K)_i|^2 + \alpha \|\overline{W}\|_1 + \beta \sum_{i} (W_i \log W_i + \overline{W_i} \log \overline{W_i}), \\ \text{s.t.} \quad W_i + \overline{W_i} = 1, \quad \left\{W_i, \overline{W_i}\right\} \in [0,1]\,. \end{gathered} \tag{9}$$

Decomposing (9) into a set of independent sub-problems, and meeting the first constraint (i.e. replacing $\overline{W_i}$ with $1 - W_i$), we have,

$$\min_{W_i} W_i |B_i - (I \otimes K)_i|^2 + \alpha(1 - W_i) + \beta(W_i \log W_i + (1 - W_i)\log(1 - W_i)). \tag{10}$$

The closed-form solution of (10) can be given as,

$$W_i = \left(\exp\left(\frac{|B_i - (I \otimes K)_i|^2 - \alpha}{\beta}\right) + 1\right)^{-1}. \tag{11}$$

Note that the solution in (11) meets the second constraint in (9) (i.e. $W_i \in [0,1]$), and it is in a standard sigmoid function form, which complies with our intuitive assumption that the probabilities of elements being outliers vary inversely with their corresponding residuals.

### 3.4 Overall algorithm

Our algorithm is implemented in a coarse-to-fine framework [3]. Since the outliers are largely removed by the down-sampling procedure, handling outliers in

**Algorithm 1:** Blind image deblurring with massive outliers

**Input:** Image pyramid $\{B_1, B_2, ..., B_n\}$ obtained by down-sampling the input image $B$ which is severely corrupted, and $B_1 = B$.

1: Estimate coarse kernels (from $K_n$ to $K_2$) by iteratively updating latent image and blur kernel without weighting matrix updating steps.

2: Upsample $K_2$ as an initial kernel for the full resolution deblurring process.

**while** *iter = 1:maxiter* **do**

  **repeat**

    3: Updating latent image using (6)

    4: Updating weighting matrix using (9)

  **until** $I_1$ *converges*;

  **repeat**

    5: Updating blur kernel using (8)

    6: Updating weighting matrix using (9)

  **until** $K_1$ *converges*;

**end**

7: With blur kernel $K$, we use the proposed non-blind deblurring method to recover the final image $I$ (i.e. conducting step 3 and 4 iteratively).

**Output:** Blur kernel $K$ and sharp image $I$.

coarse image pyramids is unnecessary [31], and thus we deblur the coarse image pyramids without the outlier detecting step. Only for the original resolution pyramid $B_1$, we apply the OID method. After the blur kernel is obtained, the sharp image is recovered by our non-blind deblurring method. The overall deblurring steps are described in Algorithm 1. Our non-blind deblurring method is by iteratively updating the latent image and weighting matrix as described in steps 3 and 4. Main steps of the proposed algorithm are illustrated in Fig. 3.

## 4 Analysis

In this section, we give more explanations of the proposed updating strategy and further provide an analysis of the effectiveness of the outlier handling method. Please refer to our supplementary material for further analyses.

### 4.1 Explanation of the updating strategy

As described in Section 3.1, our proposed updating strategy is the main reason that leads to the success of this method. Besides the intuitive explanation provided in Section 3.1, we here analyze the intrinsic differences between different strategies.

Taking the process of solving (4) for an instance. For an individual element, we here only focus on the fidelity term because it is most affected by the outlier.

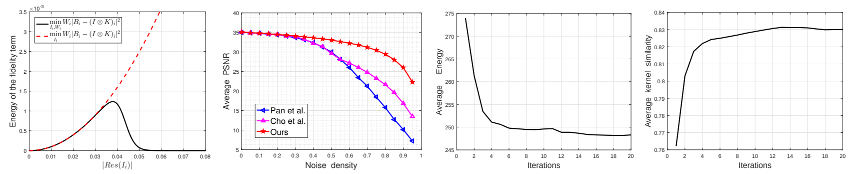


(a) (b) (c) (d)

**Fig. 4.** (a) Energies of the data fidelity term correspond to different residua value (i.e. $Res(I) = B - I \otimes K$) from different updating strategies. (b) Evaluations of different outlier handling methods [4, 22] on the dataset [16] with increasing impulsive noise (density from 0 to 0.95). (c) Average energy of (4). (d) Average kernel similarity [11].

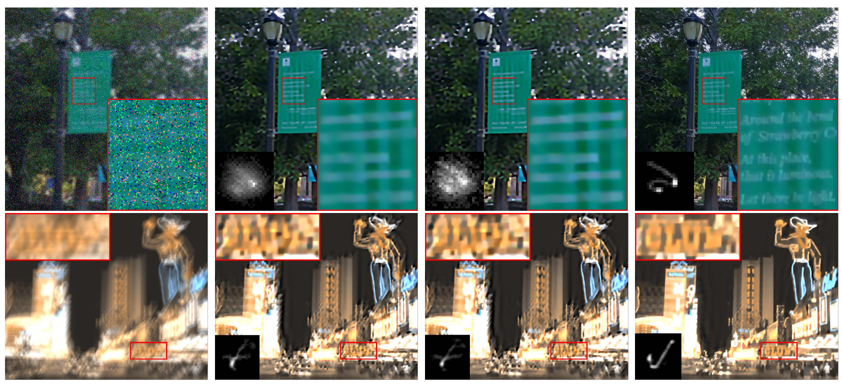

(a) Input (b) Weights fixed (c) W/O iteration (d) Ours

**Fig. 5.** Deblurring results of different updating strategies. (b) is the naive approach that iterates $\{I, K, W\}$ in a sequence. (c) is the proposed approach without inner iteration which iterates $\{W, I, W, K\}$ in a sequence.

Replacing $W_i$ with its formation in (11), we have,

$$\begin{aligned}\min_{I_i, W_i} W_i|B_i - (I \otimes K)_i|^2 &= \min_{I_i} \frac{|B_i - (I \otimes K)_i|^2}{\exp(\frac{|B_i - (I \otimes K)_i|^2 - \alpha}{\beta}) + 1} \\ &= \min_{Res(I_i)} \frac{|Res(I_i)|^2}{\exp(\frac{|Res(I_i)|^2 - \alpha}{\beta}) + 1} \\ \text{s.t.} \quad Res(I_i) &= B_i - (I \otimes K)_i.\end{aligned} \tag{12}$$

As shown in Fig. 4 (a) (black line), when the value of the residual (i.e. $Res(\cdot)$) is large enough, which is the case for salient outliers, the corresponding energy stabilizes at a small value. In this case, the polluted element does not affect the deblurring process. In another view, minimizing the energy of (12) will lead to two different solutions, for the inlier, the minimizing procedure reduces the residual to 0, which serves to smooth the residual; for the potential outlier, the solution amplifies the residual towards $+\infty$, and this solution can promote the saliency of potential outliers. These properties guarantee that inliers contribute fully while outliers are discarded during the deblurring process.

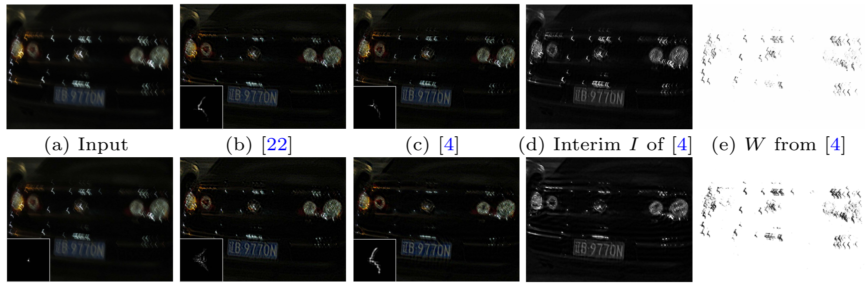

(a) Input (b) [22] (c) [4] (d) Interim $I$ of [4] (e) $W$ from [4]

(f) [5] (g) [26] (h) OID (i) Interim $I$ of OID (j) $W$ from OID

**Fig. 6.** Comparison of different outlier handling methods. Here the methods from [4] and [26] are originally designed for the non-blind deblurring task, and we extend them using the kernel updating strategy from OID.

In comparison, if the updating process is conducted while the weighting matrix is fixed, the outlier will cause a large offset for the fidelity term. As illustrated in Fig. 4 (red dot), this approach is incapable of identifying pixels according to their types (e.g. inlier or outlier) intrinsically. Besides the example given in Fig. 2, we here present another example with impulsive noise in Fig. 5. We note that both the results generated from the naive approach and the proposed method without inner iteration contain significant artifacts and residuals, while the proposed strategy generates results with clearer details and sharper edges. The results validate the effectiveness of the proposed strategy.

### 4.2 Differences from other outlier handling methods

**Relation with Dong et al. [5].** The differences between OID and [5] are as follows. First, compared with OID, the method [5] uses a more sophisticated fidelity function to inexplicitly cope with outliers. Despite the complicated formation of this strategy, it may not be appropriate for the additive noise, which will affect both the latent image and kernel updating processes during deblurring [25]. In contrast, OID adopts a more reasonable $l_2$ norm to fit the additive Gaussian noise. A real-world example in Fig. 6 shows the limitation of this model, where their result contains significant artifacts and blur residue compared to ours.

Second, this method uses the outlier detection method from [22]. Compared to the proposed outlier identifying scheme, their function is more complex yet less persuasive. We verify the effectiveness of these two outlier detecting methods by conducting non-blind deblurring experiments on the given dataset [16] with different outlier detecting strategies. As shown in Fig. 4 (b), the same MAP model with our outlier detecting skill performs more efficiently than which from [22] when there exist massive outlies (Details can be found in our supplementary material). The results explain the reason why OID performs better than [5] in blind deblurring with outliers.

**Relation with Cho et al. [4].** The method from Cho et al. [4] is mainly designed for the non-blind deblurring task. We show that with the kernel updating strategy presented in (4), this method can be easily extended for blind deblurring. As shown in Fig. 7 (b), the extension of [4] performs favorably against state-of-the-art outlier handling methods [5,22], which validates the effectiveness of the proposed kernel updating strategy.

The main difference between our approach and the extension of [4] is the selection of different outlier detecting methods. The approach [4] uses an Expectation-Maximization (EM) method to estimate outliers in the residual. Although effective on most occasions as it is, this method requires an evaluation of the outlier density before the deblurring process, which may encounter setbacks in some scenarios. Fig. 6 shows one example where the extension of [4] does not perform well. The main reason is that the outliers are not correctly detected (Fig. 6 (c)). In contrast, the proposed method detects correct outliers and generates results with fine details. Moreover, the results in Fig. 4 (b) also show that the outlier detection method from [4] is less effective than which from OID when massive outliers exist. The results validate the superiority of OID over the extension of [4].

**Relation with other outlier handling methods [22, 26].** Although Pan et al. [22] propose to explicitly identify outliers during deblurring, they only conduct the detecting process once in an iteration sequence. Their method can be viewed as the naive approach we introduce in Section 3.1. To mitigate the problem, they use an ad-hoc edge-selecting step during latent image estimation step, and they also suggest to cover more potential outlier regions during kernel estimation. Example in Fig. 6 (b) shows the ineffectiveness of this approach compared to OID when salient edges are difficult to extract.

The non-blind deblurring method from Whyte et al. [26] extends the Richardson-Lucy algorithm by specific functions, and it is designed for saturated images. We note that this method can be straightforwardly extended to blind deblurring with the kernel updating strategy from OID, where the intermediate latent image estimation derives from their proposed non-blind deconvolution methods. As shown in Fig. 6 (g), although the extension can ease the blur to some extent, it is less effective than OID.

### 4.3 Convergence of the proposed algorithm

As our algorithm involves the non-convex optimization of $l_p$ norm, a natural question is whether the model converges. We empirically evaluate the convergence property using the dataset from [16]. We compute the values of the objective function (4) and average kernel similarity [11] at the finest image scales. Results shown in Fig. 4 (b) and (c) demonstrate that our algorithm converges less than 20 iterations.

## 5 Experimental Results

The method is implemented in the MATLAB platform on a computer with an Intel Core i5 CPU and 12 GB RAM. We set $\lambda$ and $\theta$ in (3) as 0.008 and 5, while

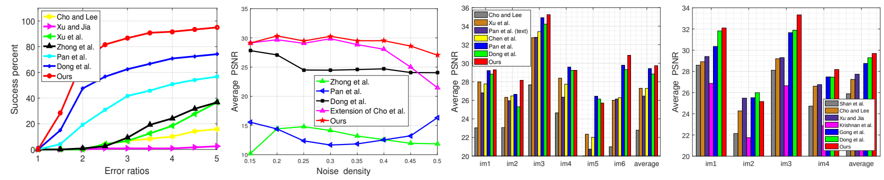


(a) (b) (c) (d)

**Fig. 7.** Quantitative evaluations with state-of-the-art methods on synthetic datasets. (a) Dataset with impulsive noise. (b) Robustness to impulsive noise. (c) Dataset with saturated pixels [21]. (d) Dataset without outliers [12].

$\alpha$ and $\beta$ are fixed as 0.0018 and 0.0002 (analyses are given in supplementary material). We empirically set the maximum iteration number (i.e. *maxiter* in Algorithm 1) to be 4 as a trade-off between speed and accuracy).

We evaluate the performance of OID on both synthetic and real images and compare it with different state-of-the-art methods. We first evaluate OID on two synthetic image datasets with different types of outliers. Then, we quantitatively test OID on two benchmark datasets [12, 16] which does not contain outliers. Finally, we examine OID on real captured images with significant outliers. To ensure fair comparisons, we use the same non-blind deblurring method introduced in Section 3.4 for all methods unless otherwise mentioned. For more examples, please refer to our supplementary material.

**Blurry images with impulsive noise:** To better demonstrate the superiority of OID, we provide a challenging image set containing 15 sharp images with a size of 800×800 and 8 blur kernels from [16], and in which we add impulsive noise with a density of 10%. Thus, a total of 120 blurry and noisy images are used to evaluate the effectiveness of different methods. Several state-of-the-art algorithms [3, 28, 29] are compared including the outlier handling methods [5, 22] and the method tailored to noise [31]. The cumulative ssd error ratio [16] is illustrated in Fig. 7 (a). OID takes lead with 69% of the results under error ration 2, while the figure for the second-best [5] is 47%.

(a) Input (b) [29] (c) [31] (d) [22] (e) [5] (f) Ours

**Fig. 8.** An example with impulsive noise.

An example from this dataset is shown in Fig. 8. Due to the effect of outliers, the conventional deblurring method [29] fails to estimate the blur kernel (Fig. 8 (b)). The method from [31] uses different filters for noise, but it is less effective when massive noise is presented (Fig. 8 (c)). Moreover, because of the significant amount of outliers, state-of-the-art outlier handling methods [5, 22] are also unable to estimate the correct blur kernels, which leads to lots of ringing artifacts

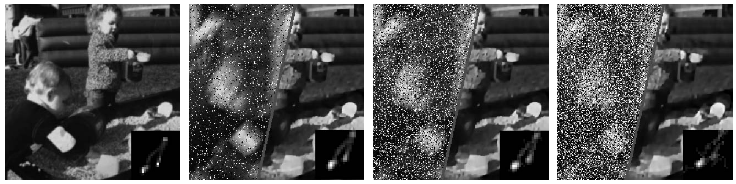

(a) (b) (c) (d)

**Fig. 9.** Deblurring results of images with increasing impulsive noises. (a) GT. (b)-(d) Images with noise densities of 0.1, 0.3, 0.5 and their corresponding results using OID.

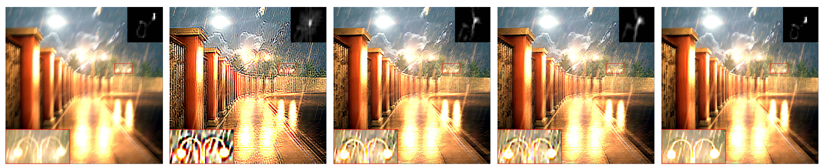

(a) Blurry input (b) [21] (c) [22] (d) [5] (e) Ours

**Fig. 10.** Comparison on a synthetic saturated regions. Results generate by our method contain finer details.

in the final recovered latent images (Fig. 8 (d) and (e)). In contrast, the blur kernel estimated by OID is visually closer to the ground truth, and the restored sharp image contains clearer details and fewer ringing artifacts (Fig. 8 (f)).

We also evaluate the proposed method using images with different densities of noise. We add impulsive noise to the dataset from [16] with increasing noise density (from 15% to 50%). Note in this test, only three methods that can handle outliers [5, 22, 31] are compared. Fig. 7 (b) shows that OID is more robust to outliers. Deblurring examples using OID are shown in Fig. 9.

**Blurry images with saturated pixels:** To further evaluate the proposed method, we test OID on a provided saturated dataset [21], which contains 6 low-light images and 8 blur kernels from [16]. We add 1% random noise to the blurry images the same as the steps in [5, 22]. We compare with 6 generic image deblurring methods [2, 3, 5, 21, 22, 29]. Note that although the method from [10] can deal with images containing saturated pixels in many cases, we do not compare with it since most images from this dataset do not contain detectable light streaks. Average PSNR values are illustrated in Fig. 7 (c). OID achieves favorable results against the state-of-the-art methods.

We also use a challenging synthetic example to demonstrate the effectiveness of the proposed method intuitively. As shown in Fig. 10, the conventional method [21] fails to deal with the blurry image contains outliers, and state-of-the-art outlier handling methods [5, 22] perform not well when given the vast scope of saturated regions. Both of these methods fail to generate blur kernels approximate to the ground truth. Consequently, the corresponding deblurring results contain lots of artifacts. In contrast, our method generates a high-quality blur kernel, and the final recovered image is more visually pleasing.

**Images without outliers:** OID can also be applied to images without outliers. We verify the effectiveness of OID by conducting experiments on the benchmark

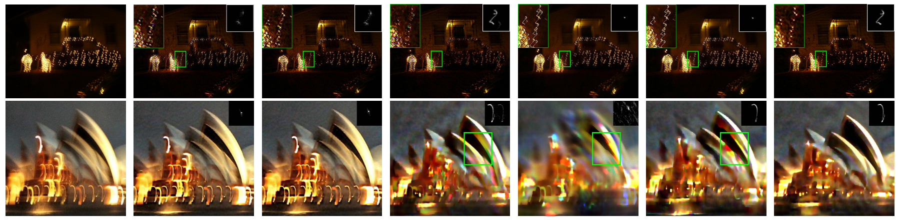

(a) Input (b) [23] (c) [2] (d) [10] (e) [22] (f) [5] (g) Ours

**Fig. 11.** Real examples contain significant outliers. The kernels estimated by our method are visually closer to the motion trajectories shown in the images (Parts eclosed in green boxes contain artifacts, best viewed on high-resolution displays with zoom-in).

dataset [12]. Average PSNR values are taken as a comparison criterion for the dataset, and the final result is shown in Fig. 7 (d). Although OID is focused on the outlier deblurring area, it also achieves comparable results against several state-of-the-art methods. Evaluation result on another benchmark dataset [16] is given in our supplementary material.

**Real-world images:** As shown in Fig. 11, state-of-the-art deblurring methods [2, 23] fail to recover sharp images due to the outliers. Although the method from [10] can extract informative light streaks in these cases, some detrimental trajectories bring side-effects to the kernel estimation processes at the same time, resulting in artifacts in final recovered images. Moreover, the outlier-handling methods [5, 22] are less effective than OID when there contain massive saturated regions. In contrast, the kernels estimated by OID are visually more similar to the light streaks appear in the blurry images, which demonstrates the effectiveness of OID.

## 6 Conclusion

In this paper, we introduce an effective framework for deblurring blurry images with massive outliers. To recap briefly, our work is based on a robust outlier identifying and discarding strategy, which enforces continuous weighting mask on elements to indicate their types. By integrating the weighting mask updating process into both the latent image and the blur kernel updating steps in an iterative manner, this strategy shows its effectiveness in identifying and penalizing outliers intrinsically. In contrast to recent art, our model does not require any heuristic edge selecting steps or sophisticated noise filtering preprocesses. Extensive evaluations on provided datasets and real images demonstrate the effectiveness of the proposed method against state-of-the-art methods.

**Acknowledgement** This work has been sponsored in part by the NSFC (No. 61731009, 61871185 and 11701079), the "Chenguang Program" supported by Shanghai Education Development Foundation and Shanghai Municipal Education Commission (17CG25), the Fundamental Research Funds for the Central Universities (No.2412020FZ023).

## References


1. Bar, L., Kiryati, N., Sochen, N.: Image deblurring in the presence of impulsive noise. International Journal of Computer Vision **70**(3), 279–298 (2006)
2. Chen, L., Fang, F., Wang, T., Zhang, G.: Blind image deblurring with local maximum gradient prior. In: IEEE CVPR (2019)
3. Cho, S., Lee, S.: Fast motion deblurring. ACM Transactions on Graphics **28**(5), 145 (2009)
4. Cho, S., Wang, J., Lee, S.: Handling outliers in non-blind image deconvolution. In: IEEE ICCV (2011)
5. Dong, J., Pan, J., Su, Z., Yang, M.H.: Blind image deblurring with outlier handling. In: IEEE ICCV (2017)
6. Dong, J., Pan, J., Sun, D., Su, Z., Yang, M.: Learning data terms for non-blind deblurring. In: ECCV (2018)
7. Fergus, R., Singh, B., Hertzmann, A., Roweis, S.T., Freeman, W.T.: Removing camera shake from a single photograph. ACM Transactions on Graphics **25**(3), 787–794 (2006)
8. Gong, D., Tan, M., Zhang, Y., van den Hengel, A., Shi, Q.: Blind image deconvolution by automatic gradient activation. In: IEEE CVPR (2016)
9. Guo, X., Lin, Z.: ROUTE: robust outlier estimation for low rank matrix recovery. In: International Joint Conference on Artificial Intelligence (2017)
10. Hu, Z., Cho, S., Wang, J., Yang, M.H.: Deblurring low-light images with light streaks. In: IEEE CVPR (2014)
11. Hu, Z., Yang, M.H.: Good regions to deblur. In: ECCV (2012)
12. Köhler, R., Hirsch, M., Mohler, B., Schölkopf, B., Harmeling, S.: Recording and playback of camera shake: Benchmarking blind deconvolution with a real-world database. In: ECCV (2012)
13. Krishnan, D., Tay, T., Fergus, R.: Blind deconvolution using a normalized sparsity measure. In: IEEE CVPR (2011)
14. Lai, W., Ding, J., Lin, Y., Chuang, Y.: Blur kernel estimation using normalized color-line priors. In: IEEE CVPR (2015)
15. Levin, A., Fergus, R., Durand, F., Freeman, W.T.: Image and depth from a conventional camera with a coded aperture. ACM Transactions on Graphics **26**(3), 70 (2007)
16. Levin, A., Weiss, Y., Durand, F., Freeman, W.T.: Understanding and evaluating blind deconvolution algorithms. In: IEEE CVPR (2009)
17. Levin, A., Weiss, Y., Durand, F., Freeman, W.T.: Efficient marginal likelihood optimization in blind deconvolution. In: IEEE CVPR (2011)
18. Li, L., Pan, J., Lai, W.S., Gao, C., Sang, N., Yang, M.H.: Learning a discriminative prior for blind image deblurring. In: IEEE CVPR (2018)
19. Liu, J., Yan, M., Zeng, T.: Surface-aware blind image deblurring. IEEE transactions on pattern analysis and machine intelligence (2019)
20. Michaeli, T., Irani, M.: Blind deblurring using internal patch recurrence. In: ECCV (2014)
21. Pan, J., Hu, Z., Su, Z., Yang, M.H.: $l_0$-regularized intensity and gradient prior for deblurring text images and beyond. IEEE Transactions on Pattern Analysis and Machine Intelligence **39**(2), 342–355 (2017)
22. Pan, J., Lin, Z., Su, Z., Yang, M.H.: Robust kernel estimation with outliers handling for image deblurring. In: IEEE CVPR (2016)

23. Pan, J., Sun, D., Pfister, H., Yang, M.H.: Blind image deblurring using dark channel prior. In: IEEE CVPR (2016)
24. Ren, W., Cao, X., Pan, J., Guo, X., Zuo, W., Yang, M.H.: Image deblurring via enhanced low-rank prior. IEEE Transactions on Image Processing **25**(7), 3426–3437 (2016)
25. Shan, Q., Jia, J., Agarwala, A.: High-quality motion deblurring from a single image. ACM Transactions on Graphics **27**(3), 73 (2008)
26. Whyte, O., Sivic, J., Zisserman, A.: Deblurring shaken and partially saturated images. International Journal of Computer Vision **110**(2), 185–201 (2014)
27. Wipf, D.P., Zhang, H.: Revisiting bayesian blind deconvolution. Journal of Machine Learning Research **15**(1), 3595–3634 (2014)
28. Xu, L., Jia, J.: Two-phase kernel estimation for robust motion deblurring. In: ECCV (2010)
29. Xu, L., Zheng, S., Jia, J.: Unnatural $l_0$ sparse representation for natural image deblurring. In: IEEE CVPR (2013)
30. Yan, Y., Ren, W., Guo, Y., Wang, R., Cao, X.: Image deblurring via extreme channels prior. In: IEEE CVPR (2017)
31. Zhong, L., Cho, S., Metaxas, D., Paris, S., Wang, J.: Handling noise in single image deblurring using directional filters. In: IEEE CVPR (2013)